Journal of GeoEngineering, Vol. 14, No. 3, pp. 155-165, September 2019
http://dx.doi.org/10.6310/jog.201909_14(3).4

APPLICATION OF POST-GROUTING IN BRIDGE FOUNDATION REINFORCEMENT: A CASE STUDY

Yanxin Yang [1], Qinke Wang [2], Jianlin Ma [3*], and Yu Fu [4]

ABSTRACT

The procedure of the post-grouting technology that improved the ultimate bearing capacity of a pile in the ShunYi Bridge foundation was introduced in this paper. In-situ static tests on two piles, pile #1 untreated by post-grouting and pile #2 treated by post-grouting, were conducted to obtain their ultimate bearing capacities. The ultimate bearing capacities were estimated based upon loading-displacement curves using the Davisson offset limit load method, Chin-Kondner method and China-code method. The nominal resistance of pile #2 was calculated by the component multiplier approach, and the improvement coefficients of the soils for the four estimation methods were used to obtain its maximum, minimum and median nominal resistances. Numerical analysis of static tests was conducted to investigate the effects of the grouting location on the ultimate bearing capacity. The results showed that the post-grouting technology improved the ultimate bearing capacity. The Davisson offset limit load method underestimated the ultimate bearing capacity of the treated pile, and the Chin-Kondner method overestimated the ultimate bearing capacity. The nominal resistance of the treated pile depended on the improvement coefficients of the soils, which were calculated based on the in-situ tests. Based on the numerical analysis, it is shown that the grouting location had a significant influence on the ultimate bearing capacity, and the ultimate bearing capacity increased if the grouting location is close to the pile tip.

Key words: Post-grouting technology, ultimate bearing capacity, bored pile, static test, numerical analysis, component multiplier approach.

1. INTRODUCTION

A large-diameter bored pile is often used as a deep foundation. However, the end bearing capacity may not be fully mobilized until the tip settlement reaches 10~15% (Mullins and Winters 2006; Bruce 1986) of the pile diameter. Because the end bearing capacity is mobilized at a large settlement, the deposits beneath the pile tip need to be treated to improve the end bearing capacity such that the design pile length can be reduced. The post-grouting technology is one of the methods that treat the soil. The post-grouting technology has been used in different engineering projects. Based on a database of static tests, Mullins (2006) proposed an empirical equation that predicts the end bearing capacity of a pile in cohesionless soil treated by post-grouting. Xiao (2009) proposed the use of the post-grouting technology in the construction project for the Beijing Capital International Airport. Gong (2009) analyzed the bearing capacity of a large-diameter pile treated by the post-grouting technology and proposed equations to calculate the bearing capacity of a treated single pile. Dai (2010) proposed an equation to calculate the bearing capacity of a treated pile, where the improvement coefficients for side and tip resistances are determined based on the statistical analysis. Yu (2011) presented a case history related to piles treated by post-grouting beneath a tower, and it was shown that the end bearing capacity was improved. Zhang (2012) investigated the behaviors of piles treated by post-grouting based on full-scale experimental tests to analyze the loading transfer mechanisms. Thiyyakkandi (2014) presented an experimental study of group piles treated by post-grouting and concluded that the post-grouting at the side and tip of the piles would increase the stiffness of the soil between the group piles. Tung (2015) summarized the applications of the post-grouting technology for bored piles and concluded that the technology could improve 50% ~ 75% of the pile bearing capacity. Wan (2017) studied the application of the post-grouting technology on coral-reef limestone and concluded that the pile bearing capacity was effectively improved. As a summary, the post-grouting technology proved to be an effective method.

The post-grouting technology is an alternative construction method with relatively low cost. The post-grouting technology has been adopted for the construction of several high-speed railway bridge foundations in China (Zou *et al.* 2010, 2011). The current paper presented the post-grouting technology used in a bridge foundation built for a new high-speed rail line. Because the preliminary design length of the bored piles is greater than 85m, the post-grouting technology was proposed to reduce the design pile length as well as the construction cost. High-pressure grouts were injected to the tip and side of the piles to increase the bearing capacity. In-situ static tests were conducted on the piles according to the Chinese Technical Code for Testing of Building Foundation Piles (Ministry of Housing and Urban-Rural Development of the PRC 2014). The bearing capacity of a treated pile was determined

Manuscript received October 2, 2018; revised March 15, 2019; accepted March 23, 2019.
[1] Ph.D. student, Department of Geotechnical Engineering, School of Civil Engineering, Southwest Jiaotong University, Chengdu, 610031, China.
[2] Ph.D. student, Department of Geotechnical Engineering, School of Civil Engineering, Southwest Jiaotong University, Chengdu, 610031, China.
[3*] Professor (corresponding author), Department of Geotechnical Engineering, School of Civil Engineering, Southwest Jiaotong University, Chengdu, 610031, China (e-mail: majianlin01@126.com).
[4] Graduate student, Department of Geotechnical Engineering, School of Civil Engineering, Southwest Jiaotong University, Chengdu, 610031, China.

based on the in-situ test results and the component multiplier approach, which is recommended by the Chinese Technical Code for Building Foundation Pile (Ministry of Housing and Urban-Rural Development of the PRC 2008). Furthermore, the finite element analysis was conducted to investigate the influences of the post-grouting location on the bearing capacity of a treated bore pile.

2. POST-GROUTING TECHNOLOGY

Due to the low-cost characteristics, the cement-based grouts are widely adopted in the construction industry. The post-grouting refers to the pile construction method that injects high-pressure grouts below the tip and at the side of a pile, as presented in Fig. 1.

During the construction of the bridge foundation mentioned in the paper, the bored piling was first conducted and then the post-grouting was conducted when the concrete strength reached more than 75% of its design strength. The grouting system consists of a cement mixer, a grouts pump, some nozzles, and several tubes that connect the grouts pump to the distribution nozzles. The crossing sonic logging tubes are attached on the side of the steel reinforcement. The tubes above the pile top are fiber braided high-pressure rubber hoses. The post-grouting system is classified as side grouting, tip grouting and combined grouting (tip and side grouting are used simultaneously) based on the location of injecting, as shown in Fig. 2.

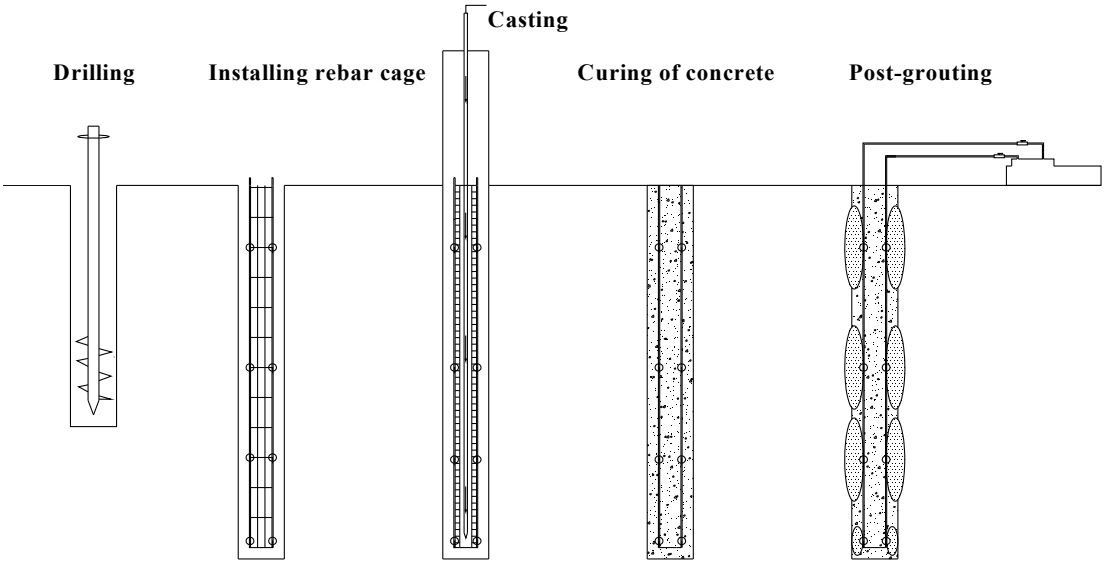

Fig. 1 Bored pile with post-grouting in details

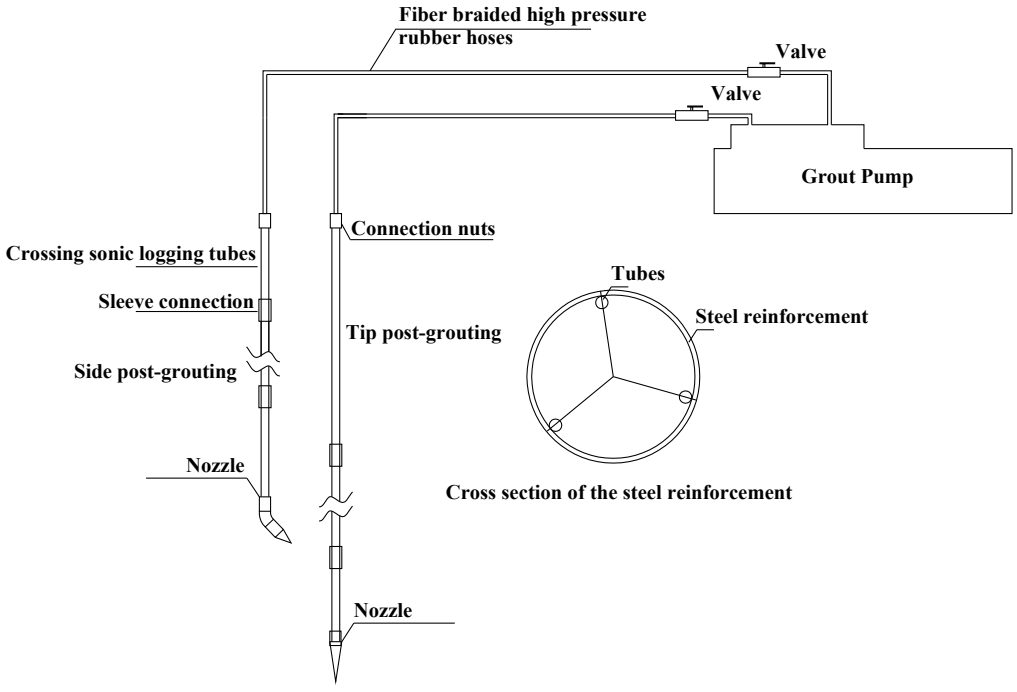

Fig. 2 Post-grouting system (side post-grouting and tip post-grouting)

3. POST-GROUTING FOR A BRIDGE FOUNDATION

ShunYi Bridge is a connection bridge built for Beijing-Shenyang high-speed railway with a 128 m long main span and two 72 m long side spans. Initially, the foundation was designed as bored piles at the bridge piers No. 189 and No. 190. However, karst caves were identified at the depth ranging from 60 m to 85 m below the ground surface, and the preliminary design pile length was 85 m in order to avoid the karst caves. To reduce the pile length and also to control the settlement, the post-grouting technology was adopted.

The site is composed of engineering filling, silty clay, silt, silty sand, and medium sand. In Fig. 3, the profile of the bored pile treated by post-grouting and the grouting locations are shown. 32 rebar strain gauges (vibrating wire type) were installed at 16 sections along the pile. The last section of the strain gauge was at the depth of 29.5 m. At each section of the pile, two gauges were placed at two points opposite to each other. Three injecting tubes, which split the section evenly, were embedded inside the section of rebar reinforcement to achieve the side post-grouting. Two injecting tubes, placed at 2 points opposite to each other, were attached outside the section of rebar reinforcement to achieve the tip post-grouting. In Table 1, the soil parameters were summarized. The ultimate unit side resistance was recommended by the Chinese Technical Code for Building Foundation Pile (Ministry of Housing and Urban-Rural Development of the PRC 2008). Silty clay-1 refers to the silty clay at the depth of −0.8 m to −3.9 m, at the depth of −18.9 m to −21.1 m, at the depth of −24.7 m to −25.9 m and at the depth of −32.1 m to deeper. Silty clay-2 refers to the silty clay at the depth of −3.9 m to −9.9 m and at the depth of −25.9 m to −30.9 m.

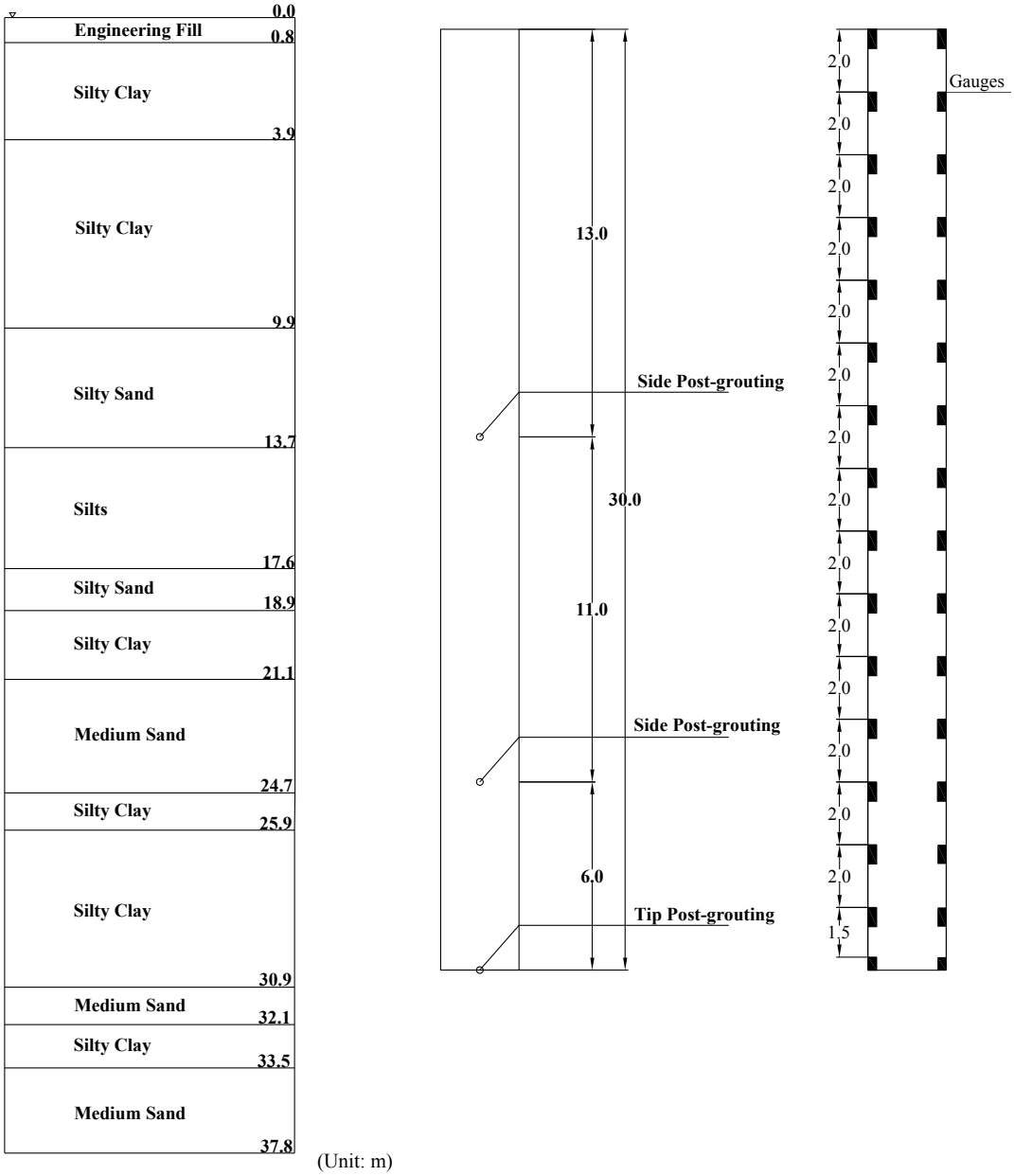

Fig. 3 The soil profile at the site, post-grouting locations and gauges layout

Table 1 Soil parameters

Soil	depth (m)	Unit weight (kN/m^3)	Cohesion (kPa)	Internal friction angle (°)	Ultimate unit side resistance (kPa)	Ultimate unit tip resistance (kPa)
Silty clay-1	−0.8 ~ −3.9 −18.9 ~ −21.1 −24.7 ~ −25.9 −32.1	19.0	15	12.5	60	800
Silty clay-2	−3.9 ~ −9.9 −25.9 ~ −30.9	19.0	17	15.0	60	800
Silts	−13.7 ~ −17.6	19.0	13	10.5	77	N.A.
Silty sand	−9.9 ~ −13.7 −17.6 ~ −18.9	20.0	13	25.0	55	N.A.
Medium sand	−21.1 ~ −24.7 −30.9 ~ −32.1	20.0	0	35.0	83	N.A.
Engineering fill	0 ~ −0.8	18.0	30	20.0	24	N.A.

4. STATIC TESTS OF THE PILES

The static tests were carried out based on the Chinese Technical Code for Testing of Building Foundation Piles (Ministry of Housing and Urban-Rural Development of the PRC 2014) to evaluate the bearing capacity and side resistance of the test piles. Test pile #2, with a diameter of 1.25 m, was treated by post-grouting, where as a reference test pile #1, with a diameter of 1.25 m, was not treated. The test site consists of 4 test piles and 7 reactions piles. Figure 4 shows the layout of the test and reaction piles. The sustained applied pressure of the grouting was 3 MPa and 0.7 MPa for the two side grouting tubes. The maximum grouting pressure was 5 MPa for the tip grouting.

The top-down loading was applied on the test pile axially, as shown in Fig. 5. The loading increments for test pile #1 and test pile #2 were 900 kN and 1900 kN, respectively. The applied loading was transferred from the measured hydraulic pressure of the jack. The displacement was measured by four LVDTs.

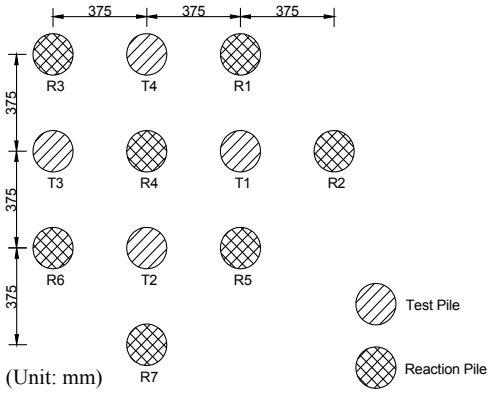

Fig. 4 Layout of the test site

Fig. 5 Load test of the top-down loading

5. INTERPRETATION OF LOADING-DISPLACEMENT CURVES

The measured loading-displacement curves for the two tests are plotted in Fig. 6. In Fig. 6, the test pile #1 failed at the loading of 14400 kN with a displacement of 29.8 mm. The loading-displacement curve of test pile #2 indicated a maximum loading of 27000 kN with a displacement of 33.52 mm.

To estimate the ultimate bearing capacities of the two piles, the Davisson offset limit load method (Davisson 1970, 1972), Chin-Kondner method (Chin 1970) and China code method (Ministry of Housing and Urban-Rural Development of the PRC 2014) were used.

As the static loading test was mandated by the China code method (Ministry of Housing and Urban-Rural Development of the PRC 2014), and the direct loading and the displacement of the pile were measured, and the measured ultimate bearing capacity could be regarded as the true value. The ultimate bearing capacity of the pile based on the China code method (Ministry of Housing and Urban-Rural Development of the PRC 2014) was used as the reference of the ultimate bearing capacity of the pile.

The Davisson offset limit load method calculated the ultimate bearing capacity by taking stiffness, length of the pile and the diameter of the pile into account. The red lines in Fig. 6 were used to estimate the ultimate bearing capacity with the Davisson offset limit load method. The Chin-Kondner method defined the ultimate bearing capacity based on the slope of the line describing the relationship between the displacement of the pile and the displacement

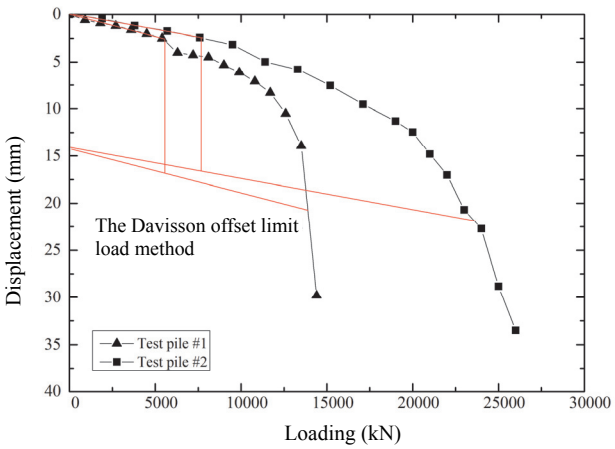

Fig. 6 The relationship between loading and displacement

divided by the applied loading. The ultimate bearing capacity of the pile was the inverse of the slope of the straight line, as shown in Fig. 7. The China code method (Ministry of Housing and Urban-the pile was the inverse of the slope of the straight line, as shown in Fig. 7. The China code method (Ministry of Housing and Urban-Rural Development of the PRC 2014) used the plot in a log-linear scale to describe the elapse time and stage loading. Several curves of the S-log(t), as plotted in Fig. 8, were used to determine the ultimate bearing capacity. When the curve changed from a level line to a line with a plunge tail, the previous stage loading was regarded as the ultimate bearing capacity.

Table 2 summarizes the estimations of the bearing capacities by the three methods. Compared to the China code method, the Chin-Kondner method predicts greater values than the applied loading on piles #1 and #2, so a safety factor for bearing capacity is needed to estimate the ultimate bearing capacity. The Davisson offset limit load method predicts smaller bearing capacities for pile #2 and greater bearing capacity for pile #1. The Davisson offset limit load method considers the equivalent elastic modulus to determine the ultimate bearing capacity when the end bearing is not fully mobilized at the beginning of the test, the ultimate bearing capacity is underestimated, so a greater downward displacement is required to mobilize the end bearing.

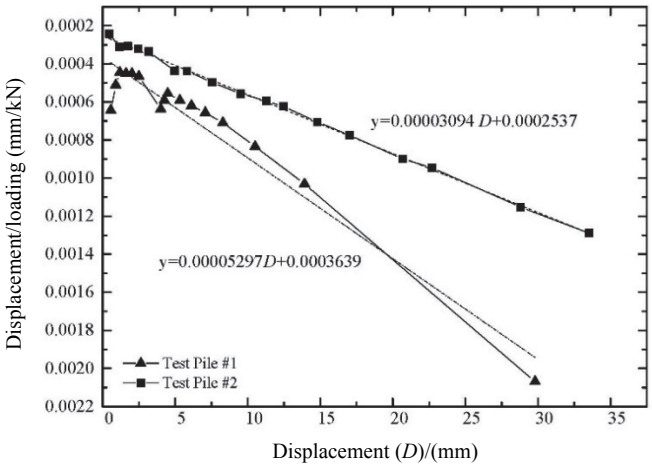

Fig. 7 Ultimate bearing capacity by Chin-Konder method

6. INTERPRETATION OF AXIAL FORCE ALONG THE PILE

In Fig. 9, the loading transferring for the load stages are shown for test piles #1 and #2, respectively. As shown in Fig. 9, the loading transferring for the test piles #1 and #2 are similar, thus the load is transferred from the uppermost stratum to the tip of the pile through the pile as the loading is increased. However, the load is transferred to the tip under different loading. In Fig. 9, the tip resistance increased dramatically when the loading was increased from 11,700 kN to 14,400 kN for pile #1, and when the loading was increased from 17,100 kN to 25,000 kN on pile #2, the tip resistance increased dramatically. For test piles #1 and #2, the loading is transferred to the pile tip under the loading of 11,700 kN and 17,100 kN, respectively. The maximum tip resistances for test piles #1 and #2 were obtained based on Fig. 9. As the ultimate bearing capacity of pile #1 and pile #2 were 13,500 kN and 25,000 kN, the maximum tip resistances for the two piles were read from the Fig. 9 as 3,402.0 kN and 3,549.0 kN, respectively. Piles #1 and #2 are friction piles based on the ratio of the tip resistance to the ultimate bearing capacity. When the loading at the top of pile #1 increased from 3,600 kN to 14,400 kN, the side resistance along the pile increased and the rate of increase was similar to pile #2, of which the loading at the pile top was increased from 1,900 kN to 11,400 kN. For pile #2, when the loading increased from 11,400 kN to 25,000 kN, the side resistance increased slowly as the ultimate side resistance was reached, and the loading was transferred from top to the tip of the pile. From the ground surface to the depth of 10m, the low contribution of the side resistance along the pile #2 was mainly due to the post-grouting location at the depth of 13 m. The grouts will form a bump in the areas adjacent to the post-grouting location, while the soil may not be improved too much from the ground surface to the depth of 10m as more grouts are pumped into the area adjacent to the grouting location at the depth of 13 m.

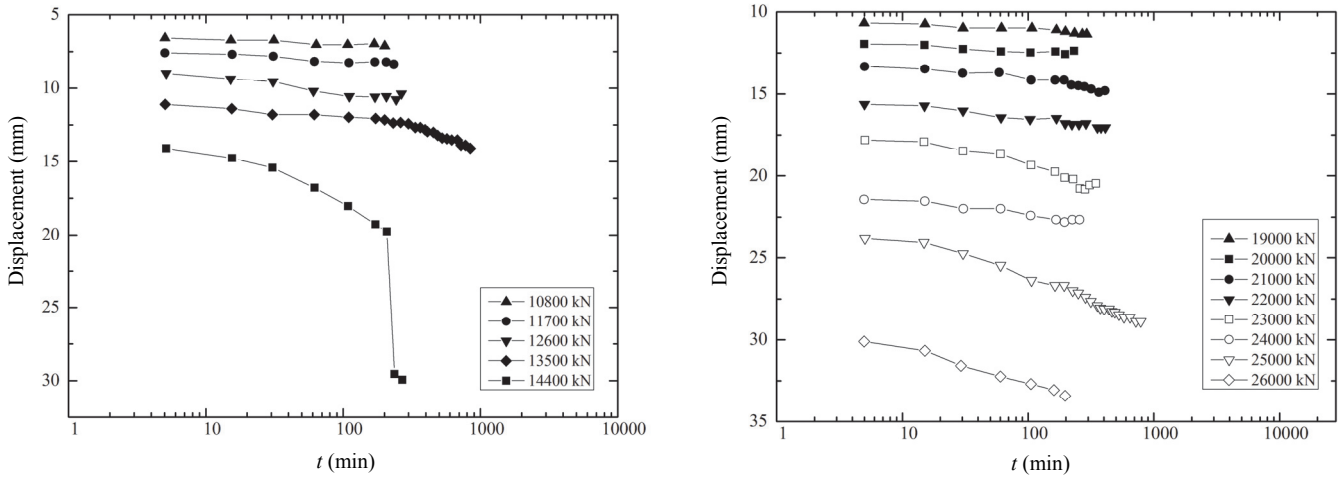

(a) S-log(t) curve of test pile #1

(b) S-log(t) curve of test pile #2

Fig. 8 Ultimate bearing capacity by China code method: (a) S-log(t) curve of test pile #1; (b) S-log(t) curve of test pile #2

Table 2 The summary of bearing capacity

Test pile	The Davisson offset limit load method (kN)	The Chin-Kondner method (kN)	The China code method (kN)
Test pile #1	13,860	18,878	13,500
Test pile #2	23,537	32,320	25,000

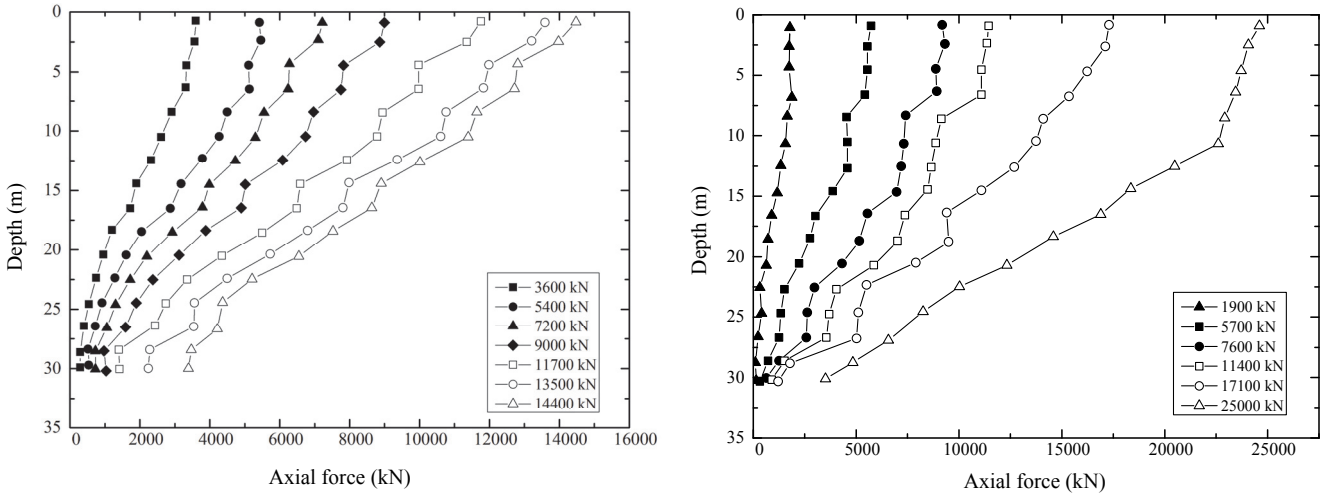

(a) Axial force distribution of test pile #1 (b) Axial force distribution of test pile #2

Fig. 9 Axial forces along the pile: (a) Test pile #1; (b) Test pile #2

7. *t-z* CURVES OF THE PILES

The single pile under axial loading was studied by the loading transfer method. The pile was discretized as a series of elements supported by nonlinear springs, and the resistance of the soil was represented by the nonlinear springs. The loading-displacement response of the pile can be obtained based on the *t-z* curve and *q-z* curve of the pile. The side resistance (t) versus displacement (z) was the nonlinear representation of the soil side reaction and the tip resistance (q) versus displacement (z) was the nonlinear representation of the soil tip reaction. To investigate the effectiveness of the post-grouting, *t-z* curves for each pile, pile #1 and #2 were plotted in Fig. 10. The soil resistance for pile #1, the soil at the depth of –30 m provided resistance less than 10 kP. When the grouts were applied, the soil resistance increased to more than 220 kPa. For both piles, the soil resistance at the depth of –28 m reached the maximum value and then decreased after the displacement passed the peak point. The *t-z* curves at the depth of –28 m identified as plastic curves. This phenomenon could also be observed at the depth of –4 m, –6 m, –14 m, –20 m, –24 m, –26 m for pile #1. For pile #2, the same phenomenon was observed at the depth of –4 m, –6 m, –8 m, –12 m, –22 m. Except for the soil at these depths mentioned above, the *t-z* curves for both piles were

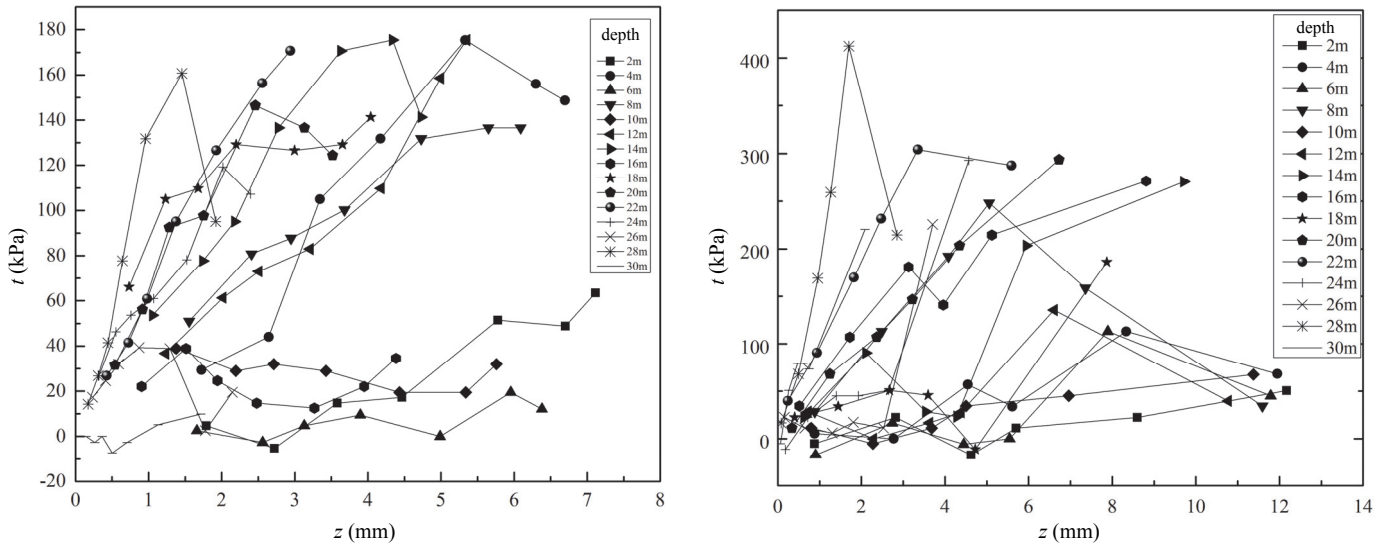

(a) The *t-z* curve of pile #1 (b) The *t-z* curve of pile #2

Fig. 10 *t-z* curves of piles

elastic curves based upon Fig. 10 for which there were no peak point. Whether the *t-z* curves tended to be elastic or plastic were mainly depending on the soil types at various depths. The effectiveness of the post-grouting was controlled by the location of the grouting. Due to the post-grouting, the soil resistance increased along the pile depth, and at the depth of −6 m, −16 m, −20 m, −24 m, −26 m, −28 m, and −30 m, the ratio of maximum soil resistance of pile #2 to the maximum soil resistance of pile #1 was greater than 1.0. While at depth of −2 m, −4 m, and −12 m, the effectiveness of the post-grouting was not obvious based on the soil resistance, and this may attribute to the locations of the post-grouting which were at 13 m below the ground surface.

8. ESTIMATION OF BEARING CAPACITY

Various methods had been developed to estimate the ultimate bearing capacity of the pile treated post-grouting, such as the tip capacity multiplier approach, the axial capacity multiplier, and the component multiplier approach and so on (Loehr *et al.* 2017). The tip capacity multiplier approach refers to the method that calculates the improvement of tip resistance by a multiplier of an improvement factor, and the axial capacity multiplier approach is based on the ultimate bearing capacity of the pile untreated with post-grouting and the improvement coefficient of the total resistance.

Different types of soil were reinforced by the post-grouting, such as cohesionless soil, clay, and rock. The effectiveness of the post-grouting depended on the soil type. For the cohesionless soil, the soil resistance could be significantly increased especially in the loose sand. In the dense sand and silty soil, the same effectiveness of post-grouting required less grout volume comparing to the loose sand. The clay required less volumes of grouts due to the cohesion of the clay. The grouting was more likely to fill the void for unsaturated clay, so equal or more volume of grouts was required for unsaturated clay comparing to the cohesionless soil. For the rock, the grouts would fill the voids and fractures of the rock, so less grouts with low pressure would be enough to increase the resistance of the rock.

To consider the side resistance and tip resistance improvement by grouting, the component multiplier approach was used to predict the nominal resistance, which was expressed in Eq. (1). The component multiplier approach was referred to as the method that was widely used in the Chinese Technical Code for Building Foundation Pile (Ministry of Housing and Urban-Rural Development of the PRC 2008). The ultimate bearing capacity of a single pile treated with post-grouting was improved at the pile tip and pile side, and the ultimate bearing capacity of a single pile was consisting of the improved ultimate tip resistance and improved ultimate side resistance. To separate the contributions of improvement to the side resistance and tip resistance, the component multiplier approach simplified the improvement by assuming each layer of soil at the site had been improved by the post-grouting. The tip resistance and side resistance of the pile were multiplied by the empirical improvement coefficients based on the soil classification and previous post-grouting projects to obtain the improved resistance of the pile. The improvement coefficient of soil resistance was defined as the ratio of measured resistance based on the in-situ tests to the ultimate resistance recommend by the Chinese Technical Code for Building Foundation Pile (Ministry of Housing and Urban-Rural Development of the PRC 2008). In the paper, to compare the pile treated post-grouting and the pile untreated with post-grouting, the ultimate bearing capacity of test pile T2 (denoted as pile #2) was presented, though four piles were tested (T1, T2, T3, T4) in Fig. 4 and three (T2, T3, T4) out of them were treated with post-grouting. Table 3 summarized the improvement coefficients for the soils evaluated by the literature. Hu *et al.* (2001) summarized the improvement coefficients of soil based on the statistical analysis of the static tests for 186 piles in 72 construction sites. The Chinese Technical Code for Building Foundation Pile (Ministry of Housing and Urban-Rural Development of the PRC 2008) mandates that the ultimate bearing capacity of the pile treated with post-grouting be determined by the static tests and the improvement coefficients were recommended in the standard. Xiao *et al.* (2009) developed the improvement coefficients based on the bored piles in Terminal 3 project of the Beijing Capital International Airport and 72 test piles rests were analyzed. Dai *et al.* (2010) developed the range of the improvement coefficients of the side resistance and tip resistance based on the Osterberg Cell loading tests of the piles in the Suramadu Bridge. The different improvement coefficients were reported in the different literature for various soil and rocks, which were limit to the specific areas. Although the improvement coefficients were developed in other engineering projects, the improvement coefficients had the potential to be used for similar soil strata in the paper to evaluate the applicability. The improvement coefficients for soil strata: silty clay, silty sand, silts, and medium sand are used to calculate the nominal resistance of the pile. As the improvement coefficient for each soil was defined as a range, the median, minimum and maximum improvement coefficients based on the coefficient range were determined based on the range. The median value, minimum value and maximum value of each improvement coefficient of the soil based upon the improvement coefficient range using the four estimation methods were then used in equation 1 to calculate the corresponding ultimate bearing capacity of the pile treated with post-grouting. In Table 4, the median value, minimum value and maximum value of the calculated ultimate bearing capacity of test pile #2 corresponding with the median, minimum and maximum improvement coefficients were presented. The median value, maximum value and minimum value of the nominal resistance based on four methods were also compared with ultimate bearing capacity by the static test.

$$Q_{uk} = u\sum q_{sjk} l_j + u\sum \beta_{si} q_{sik} l_{gi} + \beta_p q_{pk} A_P \quad (1)$$

where Q_{uk} is the ultimate bearing capacity of the pile reinforced with post-grouting technology; u is the surface area of the pile; q_{sjk} is the ultimate side resistance along the pile segment j; l_j is the length of pile segment j; β_{si} is the improvement coefficient of the side resistance at pile segment i due to post-grouting; q_{sik} is the ultimate side resistance along pile segment i due to post-grouting; l_{gi} is the length of pile segment i due to post-grouting; β_P is the improvement coefficient of the ultimate tip resistance at the pile tip; q_{pk} is the ultimate tip resistance; A_P is the cross-section area of the pile.

As the static loading test was mandated in the Chinese Technical Code for Building Foundation Pile (Ministry of Housing and Urban-Rural Development of the PRC 2008), furthermore, the test results of static loading test could be used for the development of an empirical method or calibration of the numerical model. The ultimate bearing capacity of the pile based on the China code (Ministry of Housing and Urban-Rural Development of the PRC 2008)

Table 3 Resistance improvement for the soils

Soils	Improvement coefficient							
	Hu *et al.* (2001)		Ministry of Housing and Urban-Rural Development of the PRC (2008)		Xiao *et al.* (2009)		Dai *et al.* (2010)	
	Side	Tip	Side	Tip	Side	Tip	Side	Tip
Silty clay	1.5-1.9	1.8-2.5	1.4-1.8	2.4-2.8	1.4-1.8	2.2-2.5	1.3-1.4	1.5-1.8
Silty sand	1.5-1.9		1.6-2.0		1.4-1.8		1.5-1.6	
Silts	1.3-1.5		1.2-1.3		1.4-1.8		1.3-1.4	
Medium sand	1.6-1.9		1.7-2.1		1.7-2.1		1.6-1.8	

Table 4 Nominal resistance calculated by component multiplier approach

Nominal resistance	Hu *et al.* (2001)	Ministry of Housing and Urban-Rural Development of the PRC (2008)	Xiao *et al.* (2009)	Dai *et al.* (2010)	Static test
Median value (kN)	20,937	20,934	21,035	19,020	25,000
Minimum value (kN)	19,449	19,874	19,475	18,491	
Maximum value (kN)	22,349	22,760	22,596	19,549	

was used as the reference of the ultimate bearing capacity of the pile. In Table 4, the calculated nominal resistances vary with the improvement coefficients, and all the values by the four methods are smaller than the static test result, which is the reference value. The minimum value calculated based on Dai's improvement coefficient yields the greatest error of 26.04% comparing to the ultimate bearing capacity by the static test. Among the three values by the Chinese Technical Code for Building Foundation Pile (Ministry of Housing and Urban-Rural Development of the PRC 2008), the calculated maximum value, 22760 kN, is the closest value to the static test value and the lowest error is 9.0% comparing to the static test result.

The suggested improvement coefficients by the current code Chinese Technical Code for Building Foundation Pile (Ministry of Housing and Urban-Rural Development of the PRC 2008) underestimate the nominal resistance of the site. Based on the axial force distribution of the static test, the ultimate side and tip resistances of the soil were measured when the ultimate bearing capacity of the pile was reached under the loading. For each soil layer, the unit side resistance of pile in soil was calculated based on the ratio of the measured side resistance of soil to the surface area of the pile embedded in the soil, and the unit tip resistance was calculated based on the measured tip resistance of the pile to the cross-section area of the pile. The improvement coefficients were defined as the calculated unit resistance of pile in the soil to unit resistance recommended by the Chinese Technical Code for Building Foundation Pile (Ministry of Housing and Urban-Rural Development of the PRC 2008). Table 1 showed the unit resistance of each soil recommended by the code. Based on the gauges layout along the pile depth, the mean value of unit resistance for each soil layer was obtained, and the mean value of the measured unit side resistance of silty clay is 66.0 kPa at the depth range from 0m to −10.0 m, the mean value of the measured unit side resistance of silty sand is 155.0 kPa at the depth of −10 m to −14.0 m, the mean value of the measured unit side resistance of silts at the depth from −14.0 m to −18.0 m is 229.0 kPa, the mean value of the measured unit side resistance of the silty sand at the depth of −18 m to −19 m is 294.0 kPa, the mean value of the measured unit side resistance of the silty clay at the depth of −19 m to −21 m is 288 kPa, the mean value of the medium sand at the depth from −21 m to −25 m is 259 kPa and the mean value of the measured silty clay at the depth from −25 m to −30 m is 201 kPa. The recommended mean values of the unit side resistance for silty clay, silty sand, silts and medium sand by the Chinese Technical Code for Building Foundation Pile (Ministry of Housing and Urban-Rural Development of the PRC 2008) are 60 kPa, 55 kPa, 77kPa, and 83 kPa. The improvement coefficients of side resistance, 4.1, 3.0, 3.1, and 3.5, were obtained based on the ratio of median side resistance to the recommended value by Chinese Technical Code for Building Foundation Pile (Ministry of Housing and Urban-Rural Development of the PRC 2008) for silty sand, silts, medium sand and silty clay, respectively. To obtain the improvement coefficient of the tip resistance of the silty clay, the measured ultimate tip resistance was obtained as 3,549 kN under the loading of 25,000 kN. The ratio of the unit tip resistance of 2,885 kPa to the ultimate unit tip resistance of 800 kPa recommended value by Chinese Technical Code for Building Foundation Pile (Ministry of Housing and Urban-Rural Development of the PRC 2008) for silty clay is the improvement coefficient is 3.6.

9. NUMERICAL ANALYSIS OF POST-GROUTING

A series of numerical analysis based on the site investigation was conducted to investigate the influence of the post-grouting technology on the bearing capacity of the piles using Abaqus (ABAQUS 2012). By importing or producing the geometry of the structure, the model could be created very quickly and easily. The properties of materials were assigned to the decomposed mesh of the geometry as well as the loading condition and boundary condition. The result of the analysis was visualized in the software for the interpretation.

To ensure the accuracy of the finite element model, the material parameters were used to model the static tests firstly and the

ultimate bearing capacity was compared with the in-situ test result. The loading-displacement curves were generated and compared with the static test to validate the modeling of the loading test. In addition, several positions of the post-grouting were simulated to investigate the effects of the post-grouting.

Same material properties of soil and pile were used for the simulations of the two piles. The soil and the interface between the soil and pile were simulated by the Mohr-Coulomb constitutive model. The elastic constitutive model was used to model the pile. In Table 5, the parameters used in the analysis were presented. The cohesion, internal friction angle and the unit weight of soil were obtained based on the lab test, the shear modulus and Poisson's ratio were assumed based on the typical value for each layer of soil. The material parameters of the pile and the grouts were assumed based on the typical value for each material. In Table 5, silty clay-1 referred to the silty clay at the depth of –0.8 m to –3.9 m, at the depth of –18.9 m to –21.1 m, at the depth of –24.7 m to –25.9 m and at the depth of –32.1 m to deeper, respectively. Silty clay-2 referred to the silty clay at the depth of –3.9 m to –9.9 m and at the depth of –25.9 m to –30.9 m, respectively.

The boundary condition of the model was set as: the boundary of the bottom was fixed, the boundary of the top was free, and the boundary of the free face was fixed at the horizontal direction. A half model was meshed and analyzed based on the symmetry. In Fig. 11, the meshed model of the test piles #1 and #2 were shown. To reach the initial equilibrium of the model, the initial stress was generated. In the simulation of pile treated with post-grouting, the post-grouting pressure was represented by the thermal expansion stress. The soil where the thermal expansion stress imposed was simulated with the Mohr-Coulomb constitutive model. Two methods could be used to simulate the grouts in the finite element modeling, either by enhancing the cohesion and internal friction angle of soil to simulate the grouts or by the expansion stress. Tang (2008) introduced the simulation of the pressure of post-grouting by the expansion stress. In the paper, the grouts pressure was simulated by the expansion stress. The thermal expansion could increase or decrease the volume of the element by varying the temperature and simulate the stress. By defining the Young's modulus of the grouts and expansion coefficient in the numerical modeling, a change in the temperature would bring the stress change in the model. The elements of the model expanded due to the expansion pressure and the volumes of the elements increased due to the expansion pressure. The thermal expansion stress, which was induced by the change of temperature, was equal to the post-grouting pressure imposed by a grouting volume of 5 tons and a pressure of 2 MPa. The diameter of the area, where post-grouting or thermal expansion stress was applied, was simulated as a semi-sphere with a diameter of 1.2 m.

Figure 12 showed the displacement-loading curves for the test piles #1 and #2. The simulated curves showed the same trend with the curves by the static tests. The simulated bearing capacity was less than the capacity by the static test for each curve and the initial sloping of the simulated curves were greater than the static tests. For test pile #1, the simulated curve crossed with the static test curve at some point when the axial force gradually increased. For test pile #1, the simulated curve reached at the bearing capacity of 14,400 kN at the displacement of 27.7 mm, which was smaller than 29.8 mm. In the numerical simulation, the downward displacement was not needed to mobilize the soil resistance beneath the pile, thus, smaller displacement occurred. For test pile #2, the ultimate bearing capacity was 21,042 kN at the displacement of 36.58 mm. In the simulation, the post-grouting pressure was applied on the specific area of the surrounding soil based on the injecting locations, however, the grouts were distributed unevenly along the pile in the static test, thus a smaller value of ultimate bearing capacity was obtained in the numerical simulation.

To investigate the influence of the grouting position on the ultimate bearing capacity, the grouting on the side of the pile, and at the tip of the pile were simulated using the same parameter used in the simulations of the static tests. The site was consisting of silty clay and pile. The half longitudinal section for the simulated site (as the site is a half-cylinder mesh) was shown in Fig. 13, which showed the pile embedded in one layer. The numerical mesh of pile untreated with post-grouting was also shown in Fig. 13. Figure 14 showed the displacement-loading curve of the untreated pile and the loading-displacement curves for the post-grouting at the side of the pile, thus at the level of –10 m, –15 m, –20 m, –25 m and at the pile tip corresponding with the level of –30m. The ultimate bearing capacity for the pile untreated with post-grouting was 10,972 kN corresponding with a displacement of 49.0 mm. While for the piles treated with post-grouting, the ultimate bearing capacities were 13,223 kN, 15,607 kN, 16,001 kN, 17,504 kN, and 14,135 kN when the level of the post-grouting varied from –10 m

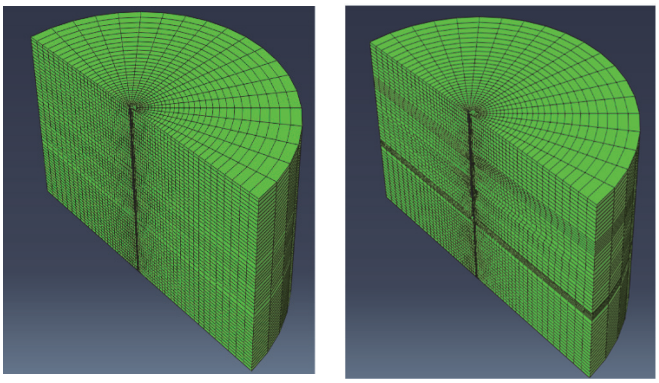

(a) The numerical mesh of test pile #1 (b) The numerical mesh of test pile #2

Fig. 11 The numerical mesh of test piles

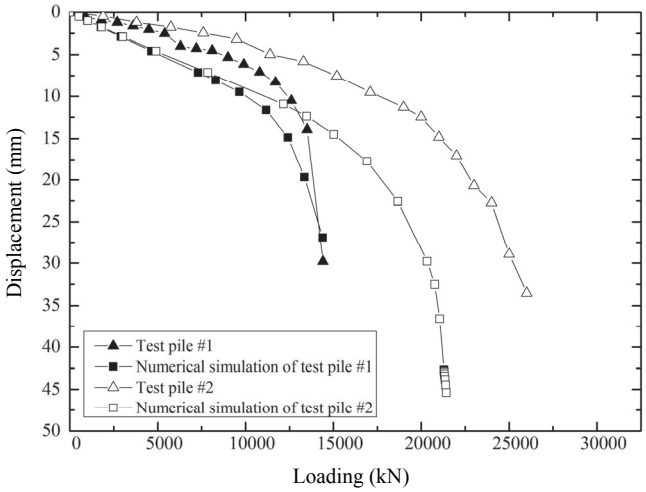

Fig. 12 The displacement-loading curves by static tests and numerical simulations

Table 5 The properties of materials used in the analysis

Materials	Unit weight (kN/m^3)	Cohesion (kPa)	Internal friction angle (°)	Shear modulus (MPa)	Poisson's ratio
Silty clay-1	19.0	15	12.5	5.0	0.30
Sily clay-2	19.0	17	15.0	13.0	0.28
Silts	19.0	13	10.5	16.0	0.28
Silty sand	20.0	13	25.0	14.0	0.26
Medium sand	20.0	1	35.0	45.0	0.25
Engineering fill	18.0	30	20.0	50.0	0.33
Post-grouting	20.0	270	40.0	700.0	0.28
Piles	25.0			30,000	0.28

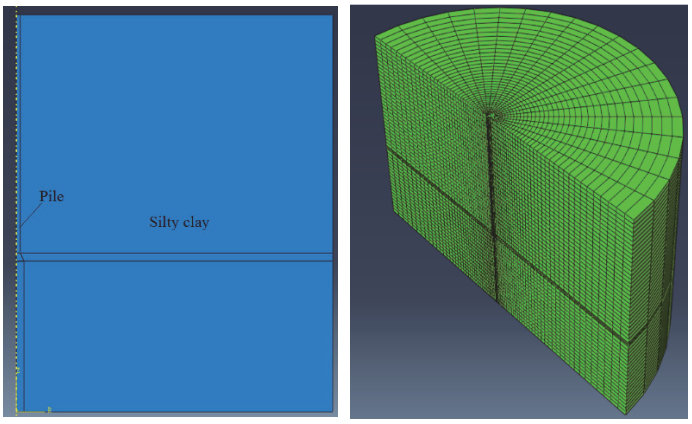

(a) Front view of the geometry (b) Numerical mesh

Fig. 13 Numerical model of pile embedded in one layer of soil (untreated pile)

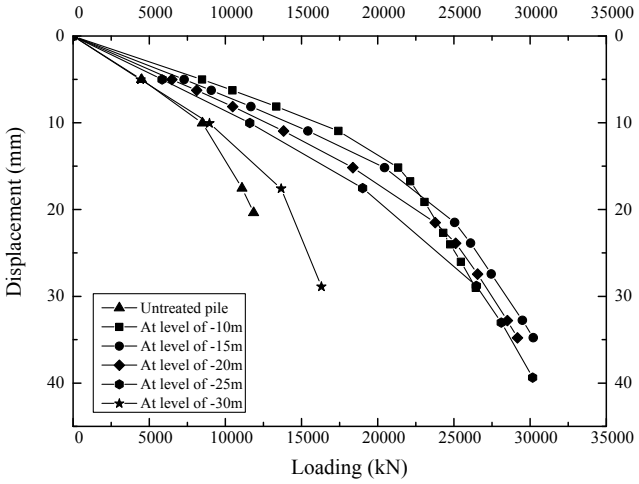

Fig. 14 The ultimate bearing capacities for the untreated pile and piles treated with post-grouting

to –30 m, respectively. The ultimate bearing capacity increased when the grouting positions moved toward the pile tip. The ultimate bearing capacity increased by a percentage of 28.8% at the pile tip, while at the side of the pile, the maximum ultimate bearing capacity increased by a percentage of 59.5%.

The difference between the effectiveness of the post-grouting at the tip and along the pile was mainly due to the grouting position and the bearing characteristic of each pile.

When the piles were classified as friction pile and end bearing pile, the location of post-grouting and the bearing characteristics of the piles were affecting the bearing capacity of the piles. The post-grouting at the pile tip was more effective for the end bearing pile, meanwhile, the post-grouting along the pile was improving the side resistance. The bearing capacity of the pile treated with post-grouting would be improved more when the grouts were applied at the tip and along the pile simultaneously. When the pile was a friction pile, the post-grouting along the pile improved the side resistance which was the main source of the bearing capacity for the friction pile. While applying the grouts at the pile tip for the long pile, the sediment beneath the pile would be removed to reduce the settlement due to the sediment. Under the situation, the post-grouting applied at the both the pile tip and along the pile were more recommended to improve the bearing capacity of the friction pile with long length.

The effect of the post-grouting was also controlled by the factors, such as the diameter of the influenced area, the pressure of the grouting, the permeability of the soil, the thickness of the soil and the others. The simulation results in the paper that the ultimate bearing capacity of the pile treated with post-grouting at a deeper depth was greater than the ultimate bearing capacity of the pile treated with post-grouting at the pile tip was due to specific site condition, the soil parameters used in the paper and other factors.

The effects of the grouting positions of piles at various levels were compared with the pile untreated with post-grouting. The post-grouting at the location close to the pile tip yielded larger ultimate bearing capacity than the other grouting locations. In the silty clay, the post-grouting improved more ultimate bearing capacity along the side of the pile than the pile tip, and the ultimate bearing capacity was likely to be increased more by the combination of post-grouting at tip and side of the pile than the post-grouting at pile tip or at the side of the pile.

10. CONCLUSIONS

Based on the reinforcement project of ShunYi Bridge foundation, the reinforcement of the post-grouting was examined and the ultimate bearing capacity of the piles were estimated based on loading-displacement curves, component multiplier approach and numerical analysis in the paper. The effects of the posting-grouting locations were further investigated with the numerical analysis.

In the in-situ tests, the piles of the foundation were treated by post-grouting. The static tests were conducted for the pile treated by post-grouting at the side and tip and the untreated pile, and the ultimate bearing capacity of the two piles were estimated and compared based on the loading-displacement curves. Three methods:

the Davisson offset limit load method, Chin-Kondner method and China code method were used to estimate the ultimate bearing capacity. Compared to the China code method, the Davisson offset limit load method underestimated the ultimate bearing capacity of pile treated by post-grouting, whereas the Chin-Konder method needed a safety factor due to the overestimation of the ultimate bearing capacity.

In order to estimate the nominal resistance of the pile treated by post-grouting, the multiplier component approach was used. The improvement coefficients of the soils of the site were estimated by four different estimation methods. The estimated nominal resistances were compared with the ultimate bearing capacity by the Chinese standard method. The comparisons showed that the estimation of nominal resistance varies with the improvement coefficients. The improvement coefficients of the soil were calculated based on the in-situ test results.

The numerical analysis of the post-grouting was conducted and the analysis results for the in-situ tests were compared with the measured curves for the validation of the numerical model. Furthermore, a numerical model of a single pile embedded in one layer of soil was analyzed, the influences of post-grouting locations were investigated. The simulation results showed that the ultimate bearing capacity had been improved due to the grouting location. When applying the post-grouting at the side of pile, the ultimate bearing capacity increased as the grouting moved toward the pile tip.

ACKNOWLEDGMENTS

The authors would like to thank the financial support from the funding: National Key Research & Development Program of China (2016YFC0802203).

REFERENCES

ABAQUS, C. (2012). *Analysis User's Manual,* Version 6.12, Dassault Systemes Simulia Corporation, Providence, Rhode Island, U.S.A.

Bruce, D.A. (1986). "Enhancing the performance of large diameter piles by grouting." *Ground Engineering*, **19**(4), 9-15. https://doi.org/10.1016/0148-9062(86)92518-0

Chin, F.K. (1970). "Estimation of the ultimate load of piles from tests not carried to failure." *Proceedings of the 2nd Southeast Asian Conference on Soil Engineering,* Singapore City, June, 81-92.

Dai, G., Gong, W., Zhao, X., and Zhou, X. (2010). "Static testing of pile-base post-grouting piles of the Suramadu bridge." *Geotechnical Testing Journal*, **34**(1), 34-49. http://doi.org/10.1520/gtj102926

Davisson, M.T. (1970). *Static Measurement of Pile Behavior, Design and Installation of Pile Foundation and Cellular Structures,* Fang, H.Y., Ed., Envo Publishing Company, 159-164.

Davisson, M.T. (1972). "High capacity piles." *Proceedings of the Lectures Series on Innovations in Foundation Constructions,* Chicago, 52.

Gong, W., Dai, G., and Zhang, H. (2009). "Experimental study on pile-end post-grouting piles for super large bridge pile foundations." *Frontiers of Architecture and Civil Engineering in China*, **3**(2), 228-233. http://doi.org/10.1007/s11709-009-0019-0

Hu, C., Li, X., and Wu, Z. (2001). "Study of vertical bearing capacity for postgrouting bored pile." *Chinese Journal of Rock Mechanics and Engineering*, **4**(20), 546-550. http://doi.org/10.3321/j.issn:1000-6915.2001.04.025

Loehr, J.E., Antonio M., and Peggy H.D., *et al* (2017). *Evaluation and Guidance Development for Post-Grouted Drilled Shafts for Highways*. No. FHWA-HIF-17-024, Federal Highway Administration, Washington, DC, United States.

Ministry of Housing and Urban-Rural Development of the PRC. (2008). *JGJ94-2008 Technical Code for Building Pile Foundation*, China Building Industry Press, Beijing, China.

Ministry of Housing and Urban-Rural Development of the PRC. (2014). *JGJ106-2014 Technical Code for Testing of Building Foundation Piles*, China Building Industry Press, Beijing, China.

Mullins, G. and Winters, D. (2006). "Predicting End Bearing Capacity of Post-Grouted Drilled Shaft in Cohesionless Soils." *Journal of Geotechnical & Geoenvironmental Engineering*, ASCE, **132**(4), 478-487. http://doi.org/10.1061/(asce)1090-0241(2006)132:4(478)

Tang, Z.W. and Zhao, C.G. (2008). "Mechanisms of Ground Heave by Grouting and Analytical Solutions & Numerical Modeling." *Rock and Soil Mechanics*, **29**(6), 1512-1516. http://doi.org/10.16285/j.rsm.2008.06.032

Thiyyakkandi, S., Mcvay, M., and Lai, P. (2014). "Experimental Group Behavior of Grouted Deep Foundations." *Geotechnical Testing Journal*, **37**(4), 621-638. http://doi.org/10.1520/gtj20130144

Tung, N.K., Li, W., Thanh, N.M., and Loi, N.X. (2015). "Application of pile bottom post-grouting technology to increase the bearing capacity of bored piles in Vietnam." *Electronic Journal of Geotechnical Engineering*, **20**(11), 4439-4454.

Wan, Z., Dai, G., and Gong, W. (2017). "Post-grouting of drilled shaft tips in coral-reef limestone formations: A case study." *Proceedings of the 27th International Ocean and Polar Engineering Conference*, San Francisco, U.S.A., June, pp. 719-725.

Xiao, D., Wu, C., and Wu, C. (2009). "Bored pile post-grouting technology and its engineering application." *Advances in Ground Improvement: Research to Practice in the United States and China*, Florida, U.S.A., 198-206.

Yu, C.H. (2011). "On Design and Construction of Pile Group Foundation of Taipei 101." *Geotechnical Engineering,* **42**(2), 56-69. http://doi.org/10.1142/9789812772480_0040

Zhang, Q.Q. and Zhang, Z.M. (2012). "Complete load transfer behavior of base-grouted bored piles." *Journal of Central South University,* **19**(7), 2037-2046. http://doi.org/10.1007/s11771-012-1242-8

Zou, L., Wu, X., and Peng, S. (2010). "Study on settlement calculation of pile group base by pile tip grouting in Beijing-Shanghai high-speed railway." *Subgrade Engineering,* **2**(2), 51-53. https://doi.org/10.3969/j.issn.1003-8825.2010.02.019

Zou, L., Wu, X., and Ma, J. (2011). "Study on numerical simulation of pile group foundation by pile tip grouting in Beijing-Shanghai high-speed railway." *Subgrade Engineering,* **2**(2), 30-33. https://doi.org/10.3969/j.issn.1003-8825.2011.02.010